

## COMMUNICATION

## Competitive amino-carboxylic hydrogen bond on a gold surface

Cite this: DOI: 10.1039/x0xx00000x

Zhijing Feng<sup>a,b</sup>, Carla Castellarin Cudia<sup>b</sup>, Luca Floreano<sup>b</sup>, Alberto Morgante<sup>a,b</sup>, Giovanni Comelli<sup>a,b</sup>, Carlo Dri<sup>a,b</sup>, Albano Cossaro<sup>b</sup>

Received 00th January 2012,

Accepted 00th January 2012

DOI: 10.1039/x0xx00000x

[www.rsc.org/](http://www.rsc.org/)

**An amino-carboxylic motif has been identified as a novel synthon in the formation of 2D hetero-organic architectures at surfaces. The well-defined interacting scheme we describe represents an ideal prototypical system for further investigations on the interaction at surfaces of the two functional groups.**

The nature of the amino-carboxylic interaction at metal surfaces is investigated by characterizing the 2D supra-molecular assembly of a carboxylic molecule, terephthalic acid (TPA), in the presence of an amino-terminated molecule, 1-Naphthylmethylamine (NMA). The description of the morphology and the chemistry of the intermolecular bonding scheme paves the way to further investigations on the amino-carboxylic interaction on surfaces and provides a novel method for steering the assembly of carboxylic molecules on surfaces.

The supramolecular assembly on surfaces has been widely investigated in the last decade as a key towards an effective device engineering at the nanoscale. Organic architectures on metal surfaces can be obtained by exploiting both covalent and non-covalent bonds between the molecules or by building metal-organic frameworks<sup>1-5</sup>. The interplay between molecule-substrate and molecule-molecule interactions drives the formation of the (hetero-)organic architectures and determines the morphological and chemical properties of the systems. A proper control on the self-assembly process is therefore the mandatory requirement to obtain systems with the desired properties. One possible strategy is to lock the molecules in a hydrogen bonded network, taking advantage of the chemical affinity between their functional groups. This approach mimics the organic 3D crystal growth mechanisms, based on the formation of supramolecular synthons<sup>6</sup>. In this context, several carboxylic molecules have been shown to assemble on surfaces in highly ordered architectures based on the formation of carboxylic homo-synthons<sup>7-11</sup>, the molecular auto-recognition

being favored by the intrinsic hydrogen donor (O-H) - acceptor (C=O) nature of the -COOH groups.

In the synthesis of 3D crystals, the carboxylic group has been successfully exploited also in the formation of hetero-synthons, with the growth of organic co-crystals based on the hydrogen bond with the amines of a second molecular species<sup>12-15</sup>.

In surface science, the amino-carboxylic affinity has been extensively exploited in the 2D homo-molecular self-assembly of amino-acids. It drives the formation of very long range ordered molecular chains with the molecules in their zwitterionic state on poorly reactive surfaces like Au(110)<sup>16,17</sup>, Au(111)<sup>18</sup>, Ag(111)<sup>1,19</sup>, whereas it is inhibited by the stronger carboxylic-substrate interaction on more reactive surfaces like Cu(110)<sup>20,21</sup>, Cu(111)<sup>19</sup> and Cu(001)<sup>22</sup>, where deprotonation of the carboxylic group occurs. Conversely, 2D hetero-organic assemblies based on the amino-carboxylic interaction have been poorly explored. We have recently shown how the chemical affinity between the two functional groups can drive the anchoring of a carboxylic molecule on top of an amino-terminated Self Assembled Monolayer, obtaining a vertically stacked hetero-organic structure<sup>23</sup>. On the other hand, we are not aware of examples of in-plane hetero-molecular coupling based on the interaction between these two groups.

Here we present a method for steering the assembly of a carboxylic molecule on surface. Our approach consists in modifying the metal substrate before the adsorption of the carboxylic molecules by depositing a second species of molecules, characterized by an amino-termination and a high surface mobility. In this way, we introduce a competitor to the well-known self-recognition of the carboxylic species, which modifies the molecular bonding scheme of the film. A similar approach has been reported in [24,25], where the amino-groups of melamine interact with the carbonyl oxygens of perylene derivatives forming a supramolecular template. To fulfil our

high-mobility requirement we adopted a small amino-terminated molecule, the NMA (Fig. 1 a), to treat the Au(111) surface before the deposition of the carboxylic species. For the latter, we have chosen to study the TPA (Fig. 2 a), whose assembly on the bare Au(111) surface represents a simple, prototypical system and has already been characterized by means of Scanning Tunneling Microscopy (STM)<sup>8</sup> and X-ray spectroscopies<sup>26</sup>. Both the preparation of the samples and the measurements have been performed under Ultra High Vacuum.

We first discuss the assembly of the NMA on Au(111). We performed several depositions at a sample temperature  $T_s \sim 280\text{K}$  followed by an annealing of the sample at higher temperatures, in the  $280 < T_{\text{anneal}} < 330\text{K}$  range. Both XPS and STM reveal that no multilayer is formed at these temperatures and that the saturation coverage is a function of  $T_{\text{anneal}}$ , the NMA SAM being denser at lower temperatures. STM images show in fact the presence of molecules in different configurations. Part of them are isolated or involved in disordered supramolecular structures, whereas a considerable fraction aggregates in  $n$ -leaf-clover shaped clusters, where  $n$  ranges between 3 and 5 with its mean value increasing with the overall coverage (see Supporting Information for further details on the observed  $\text{Au}_{\text{NMA}}$  morphologies).

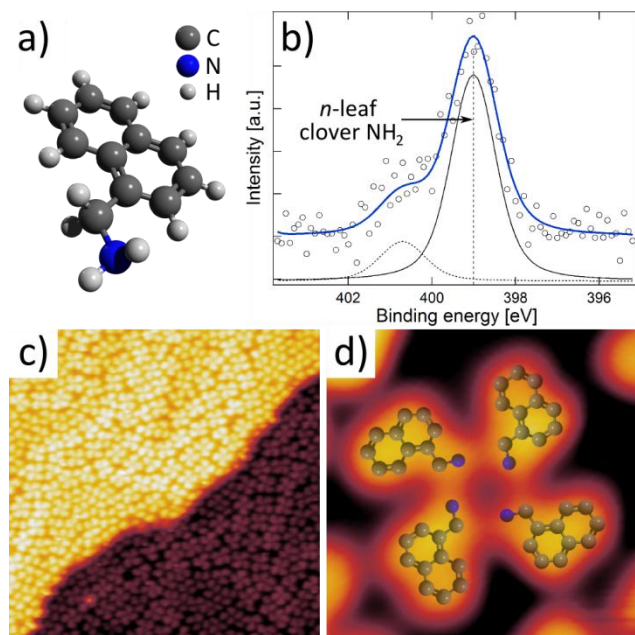


Figure 1. a) NMA molecule b) N1s XPS spectrum of the  $\text{Au}_{\text{NMA}}$  surface indicating that the amino groups of most of NMA molecules are in their neutral state. c) STM imaging of the  $\text{Au}_{\text{NMA}}$  substrate. d) 4-leaf clover of NMA. STM image parameters: (c)  $30.0 \times 30.0\text{nm}^2$ , +200mV, 20pA; (d)  $2.2 \times 2.2\text{nm}^2$ , +200mV, 30pA (hydrogen atoms are not shown in the ball and stick models).

We also observe that the same film morphologies are obtained by directly depositing the molecules on the sample kept at  $T_{\text{anneal}}$ , without any further treatment. Figure 1 reports the images of a NMA monolayer grown at Room Temperature (RT), where the four-leaf-clover is the most relevant structure at the saturation coverage. In the close-up shown in panel d) the details of this supramolecular assembly can be seen. From the

shape of the leaves, the orientation of the molecules can be inferred, indicating that the amino groups are oriented towards the center of the clover.

The N1s XPS spectrum (panel b) shows a peak with two components. The position of the main component (399.0 eV) indicates that most of the molecules are in their neutral state ( $\text{NH}_2$ ), and that therefore the intermolecular forces driving the formation of the  $n$ -leaf clover structures do not strongly affect the chemical state of the involved amines. On the other hand, the second component at 400.7 eV can be related to the presence of a minority component of molecules in a different conformation, with their amino groups interacting stronger with the substrate and/or with adjacent molecules. In fact, a shift to higher binding energies of the N1s peak can be due to the interaction of the primary amines with the gold surface<sup>27</sup> and can be related here for instance to some molecules adsorbed on the more reactive under-coordinated gold atoms at the edges of the terraces. The Au(111) surface treated with NMA ( $\text{Au}_{\text{NMA}}$ ), as reported in Fig.1, represents the initial substrate for the subsequent TPA deposition, performed at RT.

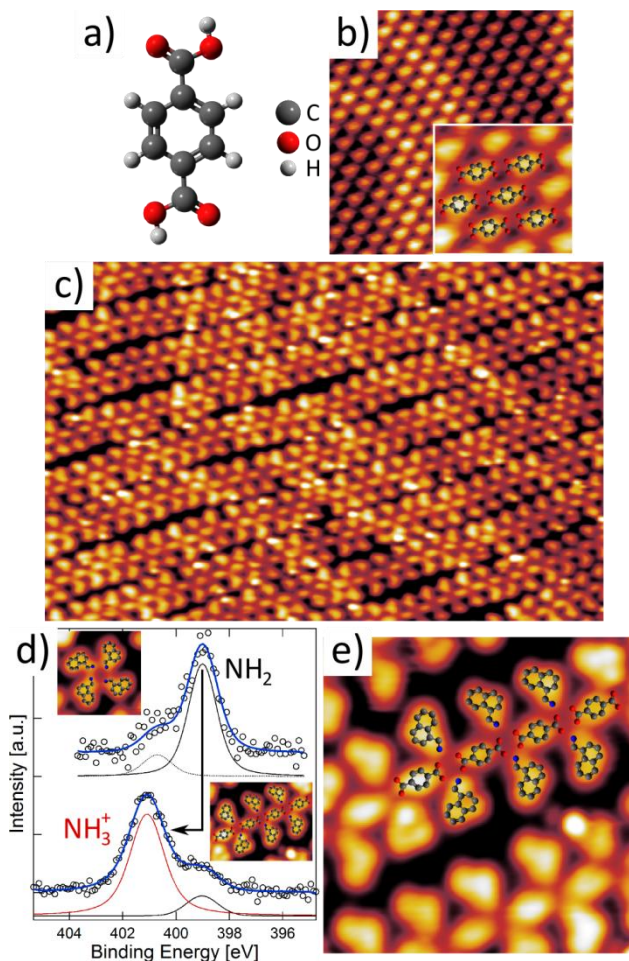


Figure 2 a) TPA molecule structure and b) its assembly on the bare Au(111) (inset shows the structure of the TPA layer) and c) the  $\text{Au}_{\text{NMA}}$  (hair-phase). d) N1s photoemission spectra show the chemical conversion of the amino-groups of NMA from neutral (already shown in Fig. 1b) to ionic state when interacting with TPA. e) Detail of the hair-like structure. STM image parameters: (b)

10.0×10.0nm<sup>2</sup>, +100mV, 500pA; (c) 29.4×18.9nm<sup>2</sup>, +200mV, 10pA; (e) 5.0×5.0nm<sup>2</sup>, +200mV, 20pA (hydrogen atoms are not shown in the ball and stick models).

Both the morphological<sup>8</sup> and the spectroscopic<sup>26</sup> properties of TPA on bare Au(111) are well known. The molecule assembles in a very compact 2D structure, formed by molecular chains placed side by side (see Fig. 2b and ref [8]), whose building block is represented by two head-to-tail aligned TPA molecules. This arrangement is driven by the hydrogen bond between the carboxylic groups, as revealed by XPS spectra. In particular, O1s spectra showed that the two non-equivalent species of oxygen atoms of the molecule are indeed involved in a donor-acceptor hydrogen bond<sup>26</sup>.

A very different situation is found upon the deposition of TPA on Au<sub>NMA</sub>, as shown in Fig 2c. It can be seen that no phase separation occurs between the two molecular species, that assemble in very long hair-like structures. The N1s XPS (Fig. 2d) shows that the amino groups of the NMA undergo a chemical conversion, the N1s binding energy now being 401.1 eV, a value compatible with the ionic NH<sub>3</sub><sup>+</sup> chemical state<sup>28</sup>. A residue of neutral component is still found at 399.0 eV. At the same time, the O1s XPS indicates that the oxygen atoms of TPA are all equivalent and the carboxylic groups are in their anionic state COO<sup>-</sup> (see Supporting Information). Therefore, both the STM imaging and XPS show that the nature of the TPA intermolecular hydrogen bond has been deeply modified by the presence of the NMA molecule.

In the STM close-up of figure 2e, the details of the hair-like structure can be distinguished and the different molecules in the structure can be easily recognized by their shape, as suggested by the superimposed ball and stick model. It can be seen that the TPA molecules are aligned in rows similar to the ones observed when TPA is adsorbed individually on the bare Au surface; here, however, two NMA molecules participate in each TPA intermolecular bond and build a novel bonding scheme. We also verified that the sample temperature during deposition plays an important role: if TPA is deposited at lower sample temperatures (T<270K) no ordered structures are observed and STM imaging is very difficult probably due to the presence of second layer molecules. We hypothesize that the mobility of the molecules in this case is too low to drive the formation of the hair-phase bonding scheme. More interestingly, both TPA deposition at higher temperature (T>330 K) or an annealing of the hair phase to the same temperature promote the formation of a hair-phase with double- or multi-TPA central rows as shown in Figure 3 (see Supporting Info for further experimental details). In fact, a minority of TPA molecules assembled in 2D structures can be found also on a surface with a highly ordered hair-phase. It can be argued that, since a 2:1 ratio between the coverage of NMA and TPA is required for the formation of the hair-phase, the formation of 2D TPA assemblies occurs when this ratio decreases towards excess TPA. Notably, the TPA assembly in the double- and triple-stranded hair reported in Fig. 3 is different from the one found on bare Au(111). The TPA rows join by aligning the phenyl groups of the molecules

instead of building the usual honeycomb structure, indicating that the NMA-TPA interaction in the outer row of the strands modifies the pairing of the inner row. Starting with even lower NMA coverage, larger 2D islands of TPA were detected, as shown in the Supporting Information.

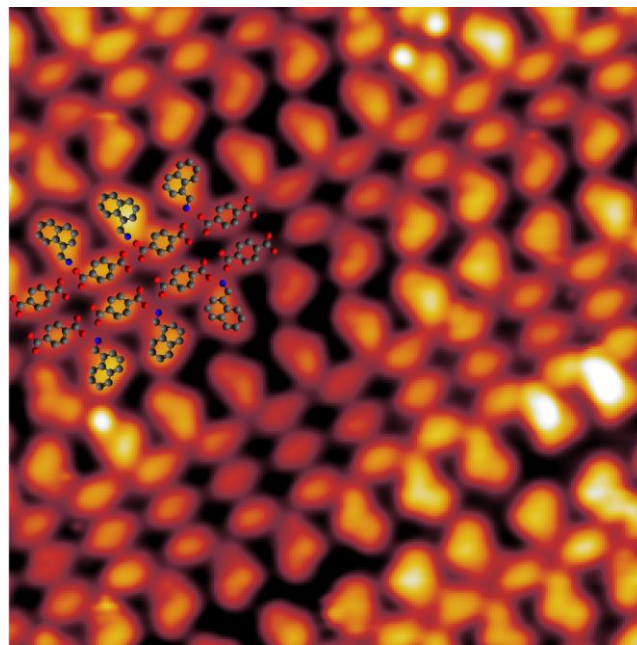


Figure 3 An excess of TPA molecules promotes the assembly of multi-stranded hair structures. The interaction with the NMA of the outer TPA molecules of the architectures also affects the pairing of the inner TPA rows. Image parameters: 9.3×9.3nm<sup>2</sup>, +200mV, 20pA (hydrogen atoms are not shown in the ball and stick models).

In conclusion, we have shown how the assembly of carboxylic molecules can be steered by treating the surface with a small amino-terminated molecule, leading to the formation of well-defined hetero-organic architectures. The amino-carboxylic chemical affinity introduces a competition in the intermolecular hydrogen bonding and determines peculiar supra-molecular assemblies. The method we developed represents a valuable opportunity to explore alternative assembly morphologies of carboxylic-terminated molecules and yields a novel amino-carboxylic motif of potential interest in the synthesis of co-crystals based on hetero-synthons. Furthermore, since these functional groups are ubiquitous in biological systems, our findings also possess a more general interest, in particular related to the study of the origin of life. Indeed, the amino-carboxylic interaction at surfaces could have played a fundamental role as a precursor in the ribosome-free peptidic bond formation in the prebiotic conditions<sup>29,30</sup>. In this context, the well-defined intermolecular scheme we found can be a convenient prototype for investigating possible routes towards the on-surface synthesis of peptides.

This work is financed by the ANCHOR project of the FIRB 2010 call of MIUR (ref. RBFR10FQBL). For the setup of the ANCHOR Lab, we acknowledge Aleksander De Luisa for the

design of the experimental chamber, Federico Salvador for collaborating in the design and in the manufacture of the variable temperature sample holder, Paolo Bertoch and Andrea Martin for the support in the setup of the mechanics and the electronics, respectively.

## Notes and references

<sup>a</sup> Department of Physics, University of Trieste, via A. Valerio 2, 34127, Trieste, Italy

<sup>b</sup> CNR-IOM Laboratorio Nazionale TASC, Basovizza SS-14, km 163.5, I-34012 Trieste, Italy e-mail: dri@iom.cnr.it, cossaro@iom.cnr.it;

† Electronic Supplementary Information (ESI) available: Experimental methods, further details about the NMA and the mixed films preparation as well as O1s photoemission evidence of the amino-carboxylic interaction are reported. See DOI: 10.1039/c000000x/

- 1 J. V Barth, *Annu. Rev. Phys. Chem.*, 2007, **58**, 375–407.
- 2 S. De Feyter and F. C. De Schryver, *Chem. Soc. Rev.*, 2003, **32**, 139–150.
- 3 L. Bartels, *Nat. Chem.*, 2010, **2**, 87–95.
- 4 L. Lafferentz, V. Eberhardt, C. Dri, C. Africh, G. Comelli, F. Esch, S. Hecht and L. Grill, *Nat. Chem.*, 2012, **4**, 215–20.
- 5 F. Cicoira, C. Santato, F. Rosei, S. Centre-ville and Q. C. Hc, *Top Curr Chem*, 2008, **285**, 203–267.
- 6 G. R. Desiraju, *Angew. Chemie Int. Ed. English*, 1995, **34**, 2311–2327.
- 7 T. Yokoyama, T. Kamikado, S. Yokoyama and S. Mashiko, *J. Chem. Phys.*, 2004, **121**, 11993–7.
- 8 S. Clair, S. Pons, A. P. Seitsonen, H. Brune, K. Kern and J. V. Barth, *J. Phys. Chem. B*, 2004, **108**, 14585–14590.
- 9 M. Lackinger and W. M. Heckl, *Langmuir*, 2009, **25**, 11307–21.
- 10 O. Ivasenko and D. F. Perepichka, *Chem. Soc. Rev.*, 2011, **40**, 191–206.
- 11 A. Carrera, L. J. Cristina, S. Bengió, a. Cossaro, a. Verdini, L. Floreano, J. D. Fuhr, J. E. Gayone and H. Ascolani, *J. Phys. Chem. C*, 2013, **117**, 17058–17065.
- 12 M. C. Etter and D. A. Adsmund, *J. Chem. Soc., Chem. Commun.*, 1990, **589**, 589–591.
- 13 O. Almarsson and M. J. Zaworotko, *Chem. Commun.*, 2004, 1889–96.
- 14 A. Mukherjee and G. R. Desiraju, *Chem. Commun.*, 2011, **47**, 4090–2.
- 15 C. B. Aakeröy, J. Desper and J. F. Urbina, *Chem. Commun.*, 2005, **6081**, 2820–2.
- 16 A. Kühnle, L. Molina, T. Linderöth, B. Hammer and F. Besenbacher, *Phys. Rev. Lett.*, 2004, **93**, 086101.
- 17 A. Cossaro, S. Terreni, O. Cavalleri, M. Prato, D. Cvetko, A. Morgante, L. Floreano and M. Canepa, *Langmuir*, 2006, **22**, 11193–11198.
- 18 V. Humblot, F. Tielens, N. B. Luque, H. Hampartsoumian and C. Me, 2014.
- 19 J. Reichert, A. Schiffrin, W. Auwärter, A. Weber-Bargioni, M. Marschall, M. Dell’Angela, D. Cvetko, G. Bavdek, A. Cossaro, A. Morgante and J. V. Barth, in *ACS Nano*, 2010, vol. 4, pp. 1218–1226.
- 20 E. M. Marti, S. M. Barlow, S. Haq and R. Raval, 2002, **501**, 191–202.
- 21 M. Nyberg, J. Hasselström, O. Karis, N. Wassdahl, M. Weinelt, A. Nilsson and L. G. M. Pettersson, *J. Chem. Phys.*, 2000, **112**, 5420.
- 22 S. Stepanow, T. Strunskus, M. Lingenfelder, A. Dmitriev, H. Spillmann, N. Lin, J. V. Barth, C. Wöll and K. Kern, *J. Phys. Chem. B*, 2004, **108**, 19392–19397.
- 23 A. Cossaro, M. Puppini, D. Cvetko, G. Kladnik, A. Verdini, M. Coreno, M. De Simone, L. Floreano and A. Morgante, *J. Phys. Chem. Lett.*, 2011, **2**, 3124–3129.
- 24 J. a Theobald, N. S. Oxtoby, M. a Phillips, N. R. Champness and P. H. Beton, *Nature*, 2003, **424**, 1029–31.
- 25 X. Sun, H. T. Jonkman and F. Silly, *Nanotechnology*, 2010, **21**, 165602.
- 26 A. Cossaro, D. Cvetko and L. Floreano, *Phys. Chem. Chem. Phys.*, 2012, **14**, 13154.
- 27 A. Cossaro, M. Dell’Angela, A. Verdini, M. Puppini, G. Kladnik, M. Coreno, M. de Simone, A. Kivimäki, D. Cvetko, M. Canepa and L. Floreano, *J. Phys. Chem. C*, 2010, **114**, 15011–15014.
- 28 K. Uvdal, P. Bodö and B. Liedberg, *J. Colloid Interface Sci.*, 1992, **149**, 162–173.
- 29 K. Ruiz-Mirazo, C. Briones and A. de la Escosura, *Chem. Rev.*, 2014, **114**, 285–366.
- 30 G. Danger, R. Plasson and R. Pascal, *Chem. Soc. Rev.*, 2012, **41**, 5416–29.